Free Space Optical Communications in Vehicular Networks Using Rectangular Guiding Models

Zeina S. Rihawi, Zaiton Abdul Mutalip, Roger J. Green, Matthew D. Higgins and Mark S. Leeson

***Abstract*—This letter introduces Free-Space Optical (FSO) Communication links in vehicular applications using potential guiding structures around a vehicle. An optical wireless communication system simulation is described which delivers received power, bandwidth, root mean square delay spread channel impulse response for purely diffuse and diffuse-specular materials with omnidirectional and directed transmitters. In the former case, a bandwidth of 225 MHz with a power deviation of 25% results at the exit. For the latter, a 75GHz bandwidth is available at best but with a power deviation of over 99% making receiver positioning critical. The impulse response is calculated using a Modified Monte Carlo algorithm taking into account up to 15 reflections. The effect of the pipe bend angle on the path loss is also presented and the simulation is supported with experimental work.**

***Index Terms*— Channel modelling, impulse response, multipath, optical wireless, intra-vehicle network.**

I. INTRODUCTION

OPTICAL wireless communication (OWC) has become established using both infrared and visible light [1-7], and the utilization of OWC in confined vehicular environments was proposed by Green *et al*. [8]. Both the doors and the vehicle frame form potential waveguiding structures that are free of sun and ambient light. Concentrating on the vehicle frame as a transmission medium, a waveguide in a vehicle can be defined by a sequence of pipes with different shapes; straight, bent, T- shaped with rectangular and circular cross sections. The rest of the paper is organized as follows: section 2 describes the environment studied and the channel mathematical model. Section 3 presents the simulation results with discussion. Section 4 shows the measurement results and concluding remarks are in section 5.

II. SYSTEM MODEL

The environment comprises as a straight rectangular cross-section pipe followed by a bend. The boundaries of the environment (reflective surfaces) are four walls while there are no reflectors in the planes representing the pipe entrance and exit. The optical source is an LED which is modelled by a position vector $\mathbf{P}_S$, a unit-length orientation vector $\widehat{\boldsymbol{O}}_S$, a power P_t, and a radiation intensity pattern $E(\phi,\theta)$, here taken to follow Lambert's cosine law [1]:

$$E(\theta) = ((n+1)/2\pi)\, P_t \cos^n(\theta) \quad \text{for } \theta \in \left[-\frac{\pi}{2}, \frac{\pi}{2}\right] \quad (1)$$

where θ is the angle between the generated ray and the source normal $\widehat{\boldsymbol{O}}_S$, n is the mode number of the radiation lobe (Lambertian,, $n = 1$ or directional, $n > 1$). The receiver (photodiode and receiving optics) is defined by position vector $\mathbf{P}_R$, unit-length orientation vector $\widehat{\mathbf{O}}_R$, area A_R, and field of view FOV. The scalar angle FOV is defined for an angle of incidence ψ (with respect to the detector normal $\widehat{\mathbf{O}}_R$) by:

$$P_R = \begin{cases} \frac{1}{d^2}\, E(\theta).A_R \cos(\psi) & \text{for } \psi \le \text{FOV} \\ 0 & \text{for } \psi \le \text{FOV} \end{cases} \quad (2)$$

where d is the distance between the source and the receiver. Reflectors are points within the environment receiving light and either absorbing or reflecting it. When a ray hits the surface, the intersection point is converted to an emitter and generates a new ray with a distribution probability equal to the reflection pattern of the surface. Surfaces which are purely diffusive follow the Lambert model [9].

$$R(\theta_0) = \rho\, P_i\, \frac{1}{\pi}\cos(\theta_0) \quad (3)$$

where ρ is the surface reflection coefficient, P_i is the incident optical power and θ_0 is the observation angle. Specular-diffusive material obeys the Phong model [7]:

$$R(\theta_i, \theta_0) = \rho\, P_i\, \frac{1}{\pi}\{r_d \cos(\theta_0) + (1 - r_d)\cos^m(\theta_0 - \theta_i)\} \quad (4)$$

where $r_d \in [0,1]$ is the percentage of incident signal that is reflected diffusely, m represents the directivity of the specular component and θ_i is the angle of incidence.

A. Channel Impulse Response

When there is a free unobstructed (Line of Sight or LOS) path between transmitter and receiver (which are a distance d apart), the signal will reach the receiver at approximately the same time [1]. The impulse response is:

$$h^{(0)}(t; S; R) \approx \frac{n+1}{2\pi} \cos^n(\theta)\, \cos(\psi)\, A_R / d^2\, V(\psi).\delta(t - d/c) \quad (5)$$

The function $V(\psi)$ is the visibility function which indicates the existence of an LOS path.

To find the impulse response resulting from multiple reflections, a Modified Monte Carlo ray tracing algorithm is applied [10]. This generates random rays from the emitter that follow the transmitter radiation pattern and then undergo several reflections after every one of which, the ray contributes to the total impulse response. The algorithm keeps

Submision date details will appear here.

The authors are with the School of Engineering, University of Warwick, Coventry, CV4 7AL, UK. (e-mail: Z.Rihawi@warwick.ac.uk).

tracing the ray until it leaves the pipe (either from the entrance or from exit) or it undergoes a defined number of reflections.

When a ray impinges on a surface, the impact point is calculated and the LOS path between the intersection point and the receiver is studied; if it exists, the contribution to impulse response is calculated depending on the surface material:

$$h^{(0)}(t; Ref; Rec) \approx E(\theta).\cos(\psi)\, A_R / d'^2\ V(\psi)\delta(t - d'/c) \quad (6)$$

where $E(\theta)$ is the surface radiation pattern and d' is the distance between the reflector and the receiver. A new ray will be generated using the Lambert model. The reflected ray power is calculated by multiplying the input power by ρ.

III. SIMULATION RESULTS AND DISCUSSION

The study concerns rectangular cross section pipes, with a range of bend angles from straight to completely right angled as illustrated in Fig.1. We have simulated the impulse responses of 14 pipe configurations divided into two cases given in Table1 by tracking 10^6 rays from a 1 W source with a resolution of 2 ps and at bending angles (θ) of 0˚,10˚,25˚, 40˚, 55˚, 70˚ and 90˚. For both pipe cases, $\hat{\mathbf{O}}_S = [0,0,1]$, $\hat{\mathbf{O}}_R = [-\sin\theta, 0, \cos\theta]$ and $\mathbf{P}_R$ consists of 25 uniformly distributed receivers over the pipe exit surface. In Case A the material is assumed purely diffusive ($n = 1$) whilst in Aluminum pipes form Case B with reflectance characteristics obtained from [11] and a directional source ($n = 505$).

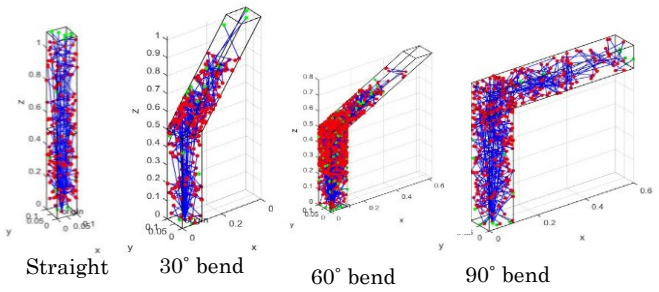

Fig 1 System configurations

Existing indoor OWC modeling studies have employed up to five reflections [6], since these contain most of the power and their computation is burdensome. However, the number of significant received reflections varies greatly dependent on, *inter alia*, materials and environment dimensions.

TABLE I
SYSTEM CONFIGURATIONS AND PARAMETERS

Parameter	Case A	Case B
Pipe dimensions (cm)	10 x10 x 110	4 x 4 x 50
ρ	0.60	0.88
r_d	1.0	0.3
m	0	250
$\mathbf{P}_R$ (cm)	[5,5,0]	[2,2,0]
A_R (mm^2)	1	7
FOV	70°	60°

As shown in Fig.2 (a), LOS channels are very unlikely in Case A except when the pipe is straight. Therefore, 10 reflections have been taken into account (15 for the right-angled pipe). The simulation of the 175 channels shows that for the channels where LOS exists, the first three reflections constitute more than 95% of the total received power on an average, while for non-LOS channels they contribute between 50% and 80% of the final value.

Fig.2 (b) represents the number of order of reflection contribution to the total received power in mixed (specular-diffusive) material. Here, a LOS path exists in the straight and the 10˚ bent pipes and reflections only occur as the bend angle increases until a right angle is approached, the effect of reflections diminishes since rays are reflected back to the transmitter due to the material characteristics meaning that receiver senses only the light coming from the first reflection.

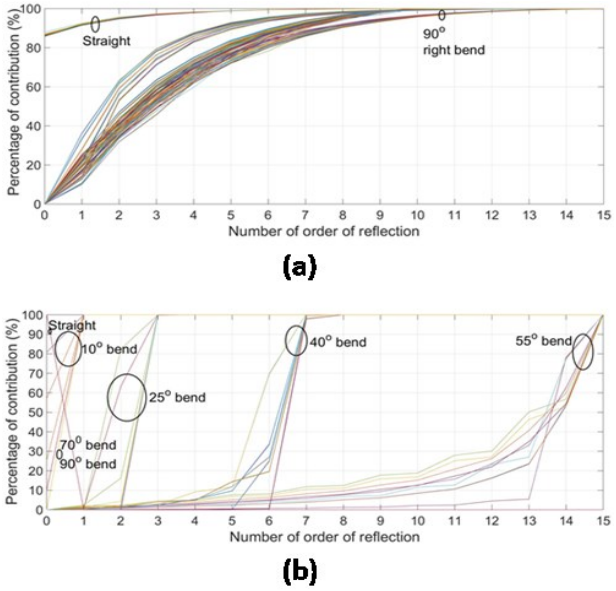

Fig. 2 Cumulative reflection contributions (a) Case A; (b) Case B

Fig. 3 illustrates the channel impulse response at two different locations in the right-angle pipe exit (corner and the center) for Cases A and B. For the former, there is significant pulse at whereas for the latter, the pulse is just delayed.

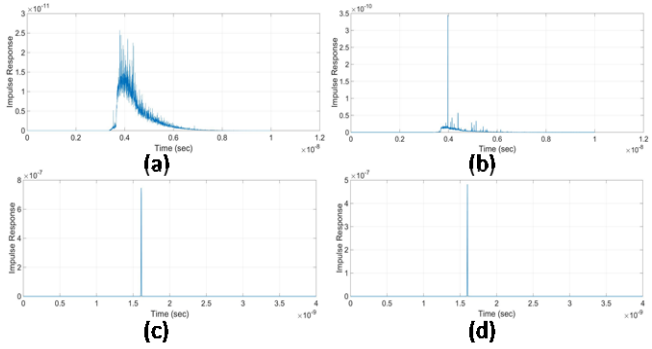

Fig. **3** Impulse response at the exit of the right angle bend pipe: Case A (a) corner (b) center; Case B (c) corner (d) center

Fig.4 (a-c) show the power distribution through the right angle bend pipe for Case A. Before the bend, the maximum

power is in the center, while directly after the bend it shifts towards the inner part of the pipe. This distribution is maintained after the bend with a drop in the value of the received power since the LOS component has been lost. At the pipe exit, the total received power varies between approximately 6 nW and 8 nW, a deviation of 25% from the peak. Similarly in Case B, shown in Fig. 5 (a-c),, the maximum power is in the center before the bend and it moves to the center line after the bend. Gradually the maximum power shifts towards the inner part of the pipe near the corner exit while the opposite corner receives negligible power. The deviation from the peak power of 1.8 μW is some 99.8%.

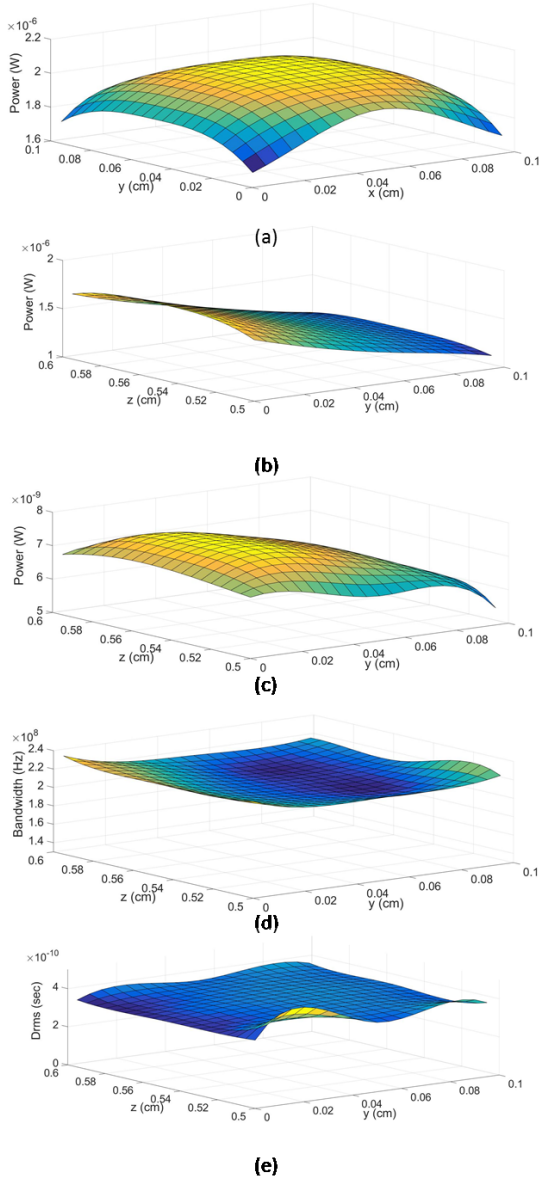

Fig. 4 Power distribution in right angle bend pipe, Case A: (a) before bend; (b) after bend; (c) at pipe exit; (d) bandwidth distribution at pipe exit; (e) $\boldsymbol{D_{\mathrm{rms}}}$ at pipe exit

The 3dB channel bandwidth is obtained by taking Fourier transform of the channel impulse response, then finding the frequency where the magnitude decreases by 3dB. Fig. 4(e) shows the bandwidth distribution over the pipe exit surface for Case A where it can be seen that the bandwidth is almost constant over the exit plane with a value equal to 225 MHz. This increases to at least 75 GHz for Case B in Fig 5 (d). In both cases, the position of maximum bandwidth is influenced by the time of travel to various positions across the exit.

The relatively small dimensions of the pipe make achieving high channel bandwidth straightforward, which means that this medium can transfer multimedia signals to the other end.

Root mean square delay spread (D_{rms}) is a useful parameter to study Inter Symbol Interference (ISI) caused by multipath distortion and is shown in Fig. 4(f) and Fig. 5 (f) across the pipe exit for Case A and Case B respectively, where:

$$D_{\mathrm{rms}} = \left[\frac{\int (t-\mu)^2 h^2(t)dt}{\int h^2(t)dt}\right]^{1/2} \tag{8}$$

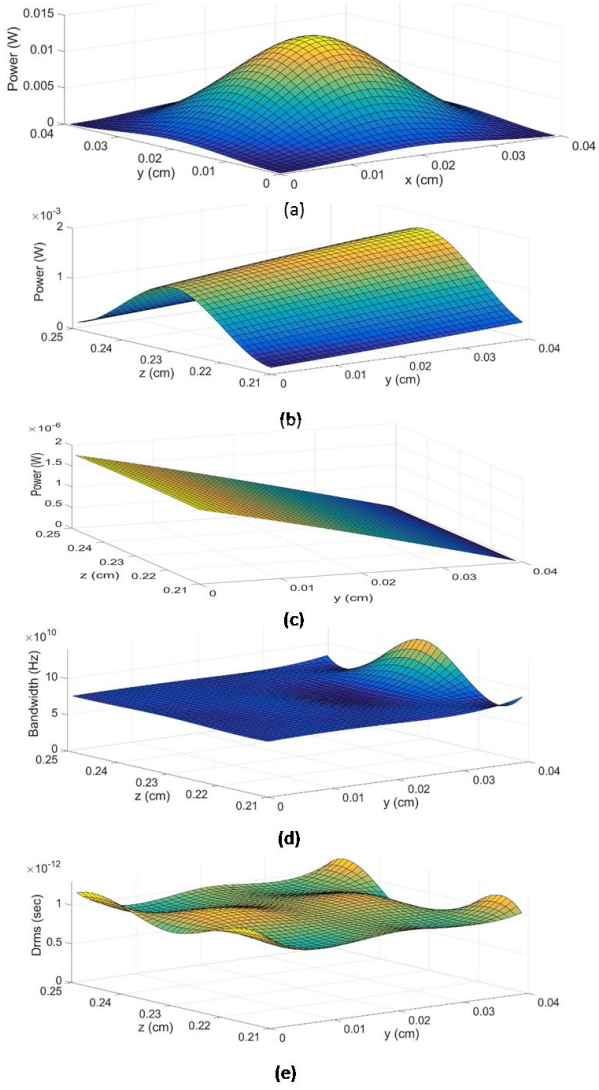

Fig. 5 Power distribution in right angle bend pipe, Case B: (a) before bend; (b) after bend; (c) at pipe exit; (d) bandwidth distribution at pipe exit; (e) D_{rms} at pipe exit

where the mean delay spread μ is given by:

$$\mu = \int t\, h^2(t)dt \Big/ \int h^2(t)dt \tag{9}$$

The limitation is the power, which drops substantially after the bend but it is possible to increase the source power without eye and skin safety concerns in the closed pipe environment. In Case A, for each bending angle the mean received power through the plane is calculated and used to find the path loss. While due to high power deviation in Case B, the maximum received power through the plane is used to represent the path loss. Fig.6 shows the path loss for different bending angles. In Case B, bending 40^o can result in better performance in terms of path loss because part of the light may reach the exit in contrast to a slightly or sharply bent pipe.

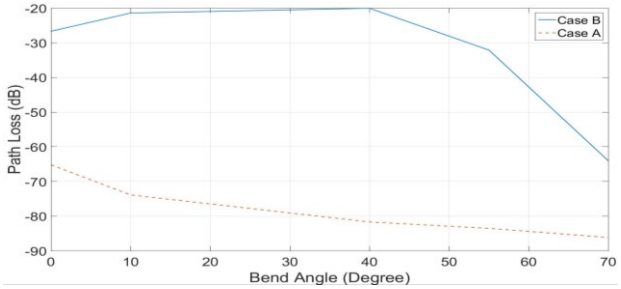

Fig. 6 Path loss vs bend degree

IV. MEASUREMENT RESULTS

Experimental support for the study was provided by power measurements of the transmission of light from a VLSY5860 IrLED (radiant intensity of 11.8 mW cm^{-2}) through a straight Aluminum rectangular guide (Case B) to a resistor-amplifier receiver with an SFH205F photodiode.

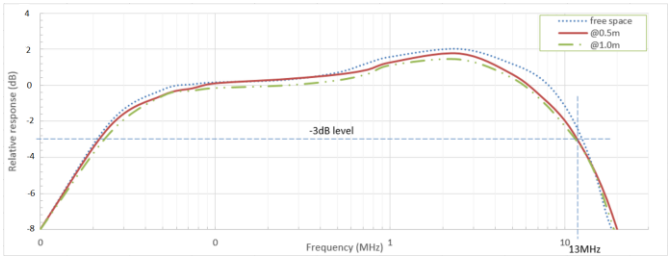

Fig. 7 Measured relative receiver response

Fig. 7 illustrates the normalized relative response of the experimental system in free space and after 0.5m and 1m within the pipe. A pre-emphasis response peak near to 2 MHz may be seen resulting from bandwidth enhancement circuitry. The -3dB bandwidth is almost unchanged by the pipe with minor amplitude differences as a result of signal reflections within it. Fig. 8 compares the simulated and measured system path losses up to 1m with good agreement obtained.

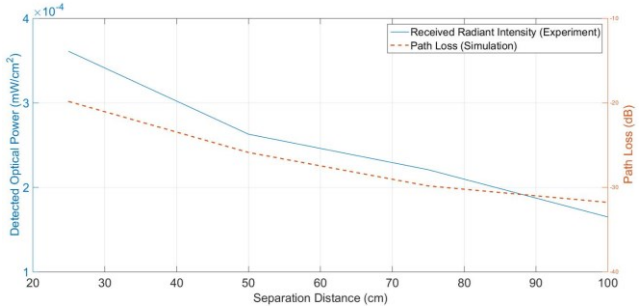

Fig. 8 Path loss and optical received power vs transmitter-receiver distance

V. CONCLUSIONS

We have employed ray tracing techniques to simulate the transmission of optical wireless signals through a new environment that can be implemented in vehicles. This initial study has focused on power distribution, bandwidth distribution and path loss in bent rectangular cross section pipes, and has also delivered channel impulse response and D_{rms} for purely diffuse and diffuse-specular materials with omnidirectional and directed transmitters. It is shown that the pipes are very plausible candidates to convey signals with appreciable bandwidth (225 MHz for diffuse material and 75 GHz for diffuse-specular material). The power deviation across the exit is relatively modest (23%) for purely diffusive material with a Lambertian source but very larger (99.8%) for diffuse-specular material with a directed source, making receiver positioning is critical. The simulations utilize 15 reflections and initial experimental results concur with them.

REFERENCES

[1] Barry J. R., *Wireless Infrared Communications*. New York, NY, USA: Springer, 1994.

[2] D. W. K. Wong and G. Chen, "Optical Design and Multipath Analysis for Broadband Optical Wireless in an Aircraft Passenger Cabin Application", *IEEE Transactions on Vehicular Technology,* vol.57, no. 6, pp. 3598 – 3606, 2008.

[3] I. Arruego, *et al*. "OWLS: A Ten-Year History in Optical Wireless Links for Intra-Satellite Communications", *IEEE Journal on Selected Areas in Communications*, vol. 27, no. 9, pp. 1599 – 1611, 2009.

[4] D. C. O'Brien, G. E. Faulkner, S. Zikic and N. P. Schmitt, "High Data-Rate Optical Wireless Communications in Passenger Aircraft: Measurements and Simulations", *6th International Symposium on Communication Systems, Networks and Digital Signal Processing,* Graz, Austria, 2008, pp. 68 - 71.

[5] N. P. Schmitt *et al.*, "Diffuse Wireless Optical Link for Air-Craft Intra-Cabin Passenger Communication", *5th International Symposium on Communication Systems, Networks and Digital Signal Processing,* Patras, Greece, 2006, pp. 625 -628.

[6] M. D. Higgins, R. J. Green and M. S. Leeson, "Mitigating the Geometrical Complexity of Intravehicle Optical Wireless Communications Systems with Wide FOV Receivers", *15th IEEE International Conference on Transparent Optical Networks*, Cartagena, Spain, 2013, paper Mo.B3.3.

[7] S. R. Perez et al., "Reflection model for calculation of the impulse response on IR-wireless indoor channels using ray-tracing algorithm", *Microwave and Optical Technology Letters*, vol. 32, no. 4, pp. 296–300, 2002.

[8] R. J. Green *et al.*, "Networks in automotive systems: the potential for Optical Wireless integration", 14th *IEEE International Conference on Transparent Optical Networks* (ICTON 2012), Coventry, UK, 2012, paper Tu.D3.1.

[9] C. R. Lomba, R. T. Valadas, and A. M. de Oliveira Duarte, "Experimental characterisation and modelling of the re flection of infrared signals on indoor surfaces," *IEE Proceedings. Optoelectronics*, vol. 145, no. 3, pp. 191–197, 1998.

[10] F. J. Lopez-Hernandez, R. Perez-Jimenez and A. Santamaria, "Modified Monte Marlo Scheme For High-Efficiency Simulation Of The Impulse Response On Diffuse IR Wireless Indoor Channels", *Electronics. Letters*, vol. 34, no. 19, pp. 1819–1820, 1998.

[11] A. M. Baldridge, S. J. Hook, C. I. Grove, G. Rivera, "The ASTER spectral library version 2.0," *Remote Sensing of Environment,* vol. 113, no. 4, pp. 711–715, 2009.